Electrochemical, Dielectric Behaviour and in Vitro Antimicrobial Activity of Polystyrene-calcium Phosphate

Tanvir Arfin[1a*], Faruq Mohammad[2b]

[1]Department of Chemistry, Uka Tarsadia University, Maliba Campus, Gopal Vidyanagar, Bardoli 394350, India

[2]Institute of Advanced Technology, Universiti Putra Malaysia, 43400 Serdang, Selangor, Malaysia

[a]*tanvirarfin@ymail.com*

Abstract: In continuation to our previous work with polystyrene-calcium phosphate (PS-CaP) composite, we further studied the conductivity behaviour under different electrolytic conditions. In the present report, the membrane potential measurements were conducted at different concentrations that ranges from 0.0001 ≤ c (M) ≤ 1 of respective salts like $BaCl_2$ and $MgCl_2$ of 2:1 electrolyte solutions at isothermal temperature (25 ± 0.1°C). The observed membrane potentials of various electrolytes follows the sequencing order of $BaCl_2$ < $MgCl_2$, confirming the cation-selective nature of the membrane. This gives an idea that the potential is a measurable parameter and can be used to characterize the charged property of the membrane. The dielectric constant decreased simultaneously with an increased frequency and also the dielectric loss tangent is shown by the complementary result with respect to dielectric constant. It is also signified from the studies that the dielectric loss tangent is directly proportional to the dielectric constant. Further, the PS-CaP material was tested for antibacterial and antifungal activity against various cultures including *Streptococcus mutans*, *Staphylococcus pyogenes*, MRSA (gram-positive bacteria), *Pseudomonas aeruginosa*, *Salmonella typhimurium*, *Escherichia coli* (gram-negative bacteria), and fungi of *Candida albicans*, *Candida krusei*, *Candida parapsilosis* and *Candida neroformans*. The result of this study concludes that the PS-CaP material has significant antimicrobial activity against all the cultures due to the chelating property and the cationic effect provided by the PS polymer.

Keywords: Polystyrene-calcium phosphate; Impedance measurements; Dielectric constant; Antimicrobial activity; Antifungal property

1 INTRODUCTION

During recent years, the increased interest of calcium phosphate [$Ca_3(PO_4)_2$; just for convenience, we refer in this report as CaP] as a necessary functional material in biomedical sector is due to its attracting physicochemical properties in addition to structural diversity, biocompatibility and biostability. The majority of CaP applications in biomedical field take the advantage of its porous structure and scaffolding character especially in orthopaedics as bone tissue engineering material and in dentistry as dental implants. When used for such applications, the biological activity of CaP helps to stimulate bone reformation and its bonding with tissues, where both are related to specific interactions of their surface with extracellular fluids and cells through various interactions of ionic exchange, superficial molecular rearrangement and

ISSN: 2222-7059(print), ISSN: 2222-7067(online), http://www.aspbs.com/aiem/
DOI: 10.7508/AIEM-V3-N3-25-38

cellular activity. The bone remodelling or renewal under the influence of CaP is modulated by the resorption of old bone mineral coupled with the new bone formation. During the resorption process, the biodegraded products from CaP bioceramics (i.e. Ca^{2+} and PO_4^{3-}) are naturally metabolized and excreted easily from the body, as observed by an increased level of the corresponding elements in urine, serum or faeces [1].

Polystyrene (PS) is an organic polymer and the ion-exchange membranes prepared by its combination with many other inorganic composites has been studied extensively [2]. The ion-exchange membranes prepared from PS finds their applications as purification or separating materials in chemical industry, food & drugs, electro dialysis, membrane electrolysis, desalination, etc. Also, these composite membranes are widely applied to the textile industry, beverages, and waste water treatment due to their high thermal, chemical and mechanical resistances [3]. When used for separation, the separation of solutes by a neutral membrane is due to the difference in sizes of solutes and their interactions with the specific membrane; however, a charged membrane separates the solutes or ions on the basis of their nature. From the viewpoint of medical and industrial sector, it is very important to thoroughly understand the ion transportation mechanism under various conditions of aqueous, organic, and electrolyte solution systems across a charged membrane [4]. For that, studying the membrane potential can be simple and highly prominent way to illustrate the transport phenomena all across a charged membrane and it is theoretically predicted as Nagasawa method which has been previously suggested by Beg *et al* [5]. The method is widely used for characterizing the ionic membranes by assuming that fixed charge groups are homogeneously distributed in the membrane throughout the surface. The charge density willingly expresses the membrane charge is calculated from the membrane potential by affecting the ion permeability of the membrane.

When the membrane has microscopic phase separated morphology and the ions preferentially permeate through one of the phases, then the degree of interconnection of the micro phase strongly influences the tortuosity of the ionic transport. Also, the dielectric properties of the membrane are one of the most important as well as systematic properties, which depend on various conditions such as the preparation method, chemical composition, sintering temperature, sintering time and doping of additives. The study of dielectric properties and electrical conductivity produces much valuable and extraordinary information on the behaviour of localized electron charge carriers which leads to greater understanding of the mechanism of the dielectric polarization in general sense [6].

The increased levels of pollution in recent years is contributing more for the microbial mediated diseases than it was during the first half of the century, and even today it is very difficult to diagnose the disease at its earlier stage. During the later-half of the century, particularly the last two decades, many different classes of antibacterial and antifungal agents were discovered to cure the microbial induced diseases [7-8]. At present, antibacterial sulfa drugs, nitrofuranes, penicillins, cephalosporins, tetracyclines, macrolides, oxaolidinones and antifungal agents such as fluconazole, ketoconazole, miconazole, amphotericin B are commonly employed against the microbial activity [7,9]. Although there has been much progress achieved towards the antibacterial and antifungal therapies where many problems has been delayed to be solved for most antimicrobial drugs that are available. For example, *Candida albicans* followed by *Candida glabrata* are the major communal pathogens that cause fungal infections in compromised patients, such as oral or gastrointestinal candidasis, urinary tract infections (mainly vulvovaginal candidiasis) [10] and systemic or bloodstream infections [11]. Therefore, it can be of significant interest to introduce alternative antifungal agents which might decrease or inhibit fungal adhesion capacity that prevents the colonization and infection by the Candida species.

By keeping in view, the present study aimed to introduce a PS-based biomaterial platform to serve as an ionic membrane with antimicrobial properties. For that, we carried the synthesis of a novel compound from PS and CaP by a sol-gel method and studied the electrochemical potential, dielectric properties and antimicrobial activity against different species of bacteria and fungi. The charge density was derived and formulated to calculate the membrane potentials of varying electrolyte concentrations by applying Nagasawa's method for electrochemical parameters.

2 NAGASAWA THEORY FOR MEMBRANE CHARGE DENSITY

Nagasawa and his co-workers [12] derived the eq. (1) shown below for the membrane potential which is existing through a negatively charged membrane. Here in this context, it is considered that there is a cell in which a membrane is separating the two aqueous solutions of varying concentrations such

as C_1 and C_2 in mol L^{-1} of an electrolyte. The solutions on both sides of the membrane are maintained for the same pressure and temperature corresponding to the electrolyte. The fluxes of water and ions relating to the cell in which the membrane is separated may be expressed by the linear equations as below:

$$-J_0 = L_{00}\,grad\,\mu_0 + L_{0+}\,grad\,\mu_+ + L_{0-}\,grad\,\mu_- \quad (1a)$$

$$-J_+ = L_{+0}\,grad\,\mu_0 + L_{++}\,grad\,\mu_+ + L_{0+}\,grad\,\mu_- \quad (1b)$$

$$-J_- = L_{-0}\,grad\,\mu_0 + L_{-+}\,grad\,\mu_+ + L_{--}\,grad\,\mu_- \quad (1c)$$

where, subscripts +, -, and *0* refer to cation, anion, and water molecules respectively, J_s corresponds to the mass fluxes (mol m^{-2} s^{-1}), L_s as the phenomenological coefficients, and μ_s as the chemical potentials. By substituting eq. (1a) into eq. (1b) and eq. (1c), we get the new eq. as followed:

$$-J_+ = -\left(\frac{L_{+0}}{L_{00}}\right)J_0 + \left(L_{++} - \frac{L_{+0}L_{0+}}{L_{00}}\right)\times grad\,\mu_+ + \left(L_{+-} - \frac{L_{+0}L_{0-}}{L_{00}}\right)grad\,\mu_- \quad (2a)$$

$$-J_- = -\left(\frac{L_{-0}}{L_{00}}\right)J_0 + \left(L_{-+} - \frac{L_{-+}L_{0+}}{L_{00}}\right)\times grad\,\mu_+ + \left(L_{--} - \frac{L_{-0}L_{0-}}{L_{00}}\right)grad\,\mu_- \quad (2b)$$

The Equations (2a) and (2b) may be approximated as the following equation given below:

$$-J_+ = -\left(\frac{C_- + X}{C_0}\right)J_0 + \left(C_- + X\right)U\,grad\,\mu_+ \quad (3a)$$

$$-J_- = -\left(\frac{C_-}{C_0}\right)J_0 + C_-V\,grad\,\mu_- \quad (3b)$$

The above two equations (3a) and (3b) are the Nernst-Planck equations which are indicating the contribution of flowing water. Where C_- is referring the effective concentration of counter ions, X as the concentration of charge, and U and V as the mobility in the membrane phase.

It is believed that the most common rate-determining step for the permeation of ions where water is the mass transfer in the membrane phase of the cell and the electrolyte solutions inside and outside of the membrane are following the concept of thermodynamic equilibrium on both sides of the membrane. This assumption is generally valid for thick membranes only. If the current does not exist at a steady state, i.e. $J_+ = J_- = J_s$ for 1-1 electrolytes and final eq. is taken as [13]:

$$-Fgrad\,\psi = -\left(\frac{J_0}{C_0}\right)\frac{X}{(C_- + X)U + C_-V} + \frac{(C_- + X)U}{(C_- + X)U + C_-V}grad\,\mu_+ - \frac{C_-V}{(C_- + X)U + C_-V}grad\,\mu_- \quad (4)$$

Substituting eq. (4) into eq. (3), we obtain

$$-J_s = -\left(\frac{J_0}{C_0}\right)\frac{C_-(C_- + X)(U + V)}{(C_- + X)U + C_-V} + \frac{C_-(C_- + X)UV}{(C_- + X)U + C_-V}grad\left(\mu_+ + \mu_-\right) \quad (5)$$

3 EXPERIMENTAL METHODS

3.1 Materials and solutions

Pure crystalline polystyrene (99.98%, Sigma-Aldrich) was used as a binder, which was finely grounded and sieved through 75 μ m. A 0.2 M sodium phosphate (99.98%, Merck chemicals) solution and a 0.2 M calcium chloride (99.98%, Sigma-Aldrich) solution were prepared for the experimentation. All other chemicals taken were of analytical grade which were specifically used.

3.2 Synthesis of PS-CaP composite membrane

For the synthesis of PS-based CaP composite membrane, we first prepared the CaP composite material by mixing 0.2 M calcium chloride solution with 0.2 M tri-sodium phosphate solution. The reaction mixture was adjusted to a pH of 1.0 by adding dilute HCl (32%, Merck chemicals) to the respective precipitate while stirring continuously at 90°C for 1 h. The resulting precipitate was washed thoroughly with demineralised water and dried at the temperature of 100°C for about 5 h in a vacuum oven (Binder VD25).

In the following step, the PS-doped composite membrane was prepared by the procedure described in our previous report [14]. Briefly, the CaP precipitate having ion-exchange property obtained in the first step was mixed with PS granules having the size less than 200 meshes and

pressed under suitable conditions of 200°C temperature and 5 ton/cm^2 pressure. In order to equilibrate the reaction components, the composite mixture was placed in a vacuum oven at a temperature of 200±0.1°C for about 30 min. All the membranes were prepared in the same way i.e. by placing the composite into the pellets and then by employing hydraulic press (Carver Hydraulic Unit Model 3912, Wabash, USA).

3.3 Measurement of membrane bi-univalent (2:1) ionic (electrolyte) potentials

The test cell used for the measurement of electrochemical potentials is similar to that of as described elsewhere [15]. The membranes were tightly clamped as a sandwich between two glass half-cells of the membrane potential for the precaution. The volume of each half-cell is 50 mL and the effective area of the membrane is 196.7 mm^2. Different electrolyte solutions such as chlorides of K^+, Na^+, and Li^+ were prepared by using deionised water specifically. A magnetic stirrer was placed and used continuously at the bottom of each half-cell in order to minimize the concentration-polarization at the surface of membrane and the measurements of the solutions were carried out gently at a stirring rate of around 500 rpm [16]. The pH of the solutions was found to be in the range of 5.5 to 6. The measurement of electrochemical potentials across the membrane was carried out randomly by adopting one of the qualitative methods which was followed at isothermal temperature condition of 25±0.2°C. These temperature conditions were maintained consistently by enhancing the refrigerated thermostat (Julabo F12-ED) [17]. The potential through the membrane was recorded persistently which have been employed at a digital multi-meter (T235H, Hellermann Tyton) by using two reference electrodes (RE) from the Radiometer analytical [18]. During each experiment, a total of three individual measurements of the membrane potential were recorded and the mean of those values were taken as the desired potential.

3.4 Membrane dielectric and impedance measurements

The dielectric constant and impedance measurements were analytically observed by utilizing Agilent-4284A precision LCR meter in the frequency range of 75 KHz–5 MHz at room temperature. The sample was fitted with circular pellets and coated by silver paste on adjacent sides, which forms a parallel plate capacitor geometry after which the values of Z, θ and C_p were estimated. With the help of the observed data, different dielectric parameters were calculated.

3.5 PS-CaP treated in vitro antimicrobial assay

The PS-CaP composite was tested for highly organised antimicrobial activity using the disk diffusion assay against some gram-positive, gram-negative strains of bacteria and fungi. Further, the zone of inhibition and minimum inhibitory concentration (MIC) i.e. the lowest concentration of the antimicrobial agent required to inhibit the visible growth of microbial strains were determined.

The *in vitro* antibacterial and antifungal activity of the PS-CaP composite tested cultures includes the gram-positive bacteria of *S. mutants, P. aeruginosa,* Methicillin resistant *staphylococcus aureus* (MRSA +ve) and gram-negative cultures of *S. pyogenes, S. typhimurium, E. coli* and the fungi of *Candida albicans, Candida krusei, Candida parapsilosis, Cryptococcus neoformans*. The inoculums of gram-positive and gram-negative bacterial cultures were prepared using the Brain-heart infusion (BHI) medium, while Sabouraud dextrose broth medium was used for the fungi and the incubation period was taken as 24 h at 37ºC temperature. The preparation of test cultures, solutions and the treatments were in accordance with McFarland protocol. The PS-CaP composite treated antibacterial and antifungal studies involved in the determination of zones of inhibition and MIC of the ligand where the complexes were determined in a sequencing way. In case of bacterial strains, Chloramphenicol (30 μg) was used as positive control and in case of fungal strains, Fluconazole (30 μg) was used as the positive control, as they both found to be involved for enhanced antimicrobial and antifungal activities respectively [19-20]. A 1 mg of each test PS-CaP composite dissolved in 100 μL DMSO (dimethlysulfoxide), a solvent generally used as an industrial solvent for the herbicides, fungicides and pesticides to get ready stock solution. From this stock solution, different concentrations of the PS-CaP composite by means of serial dilution were prepared for the treatment. For both cultures of bacteria and fungi, the disc poured in DMSO was used as the negative control. The MIC was assessed by the macro dilution test which was used to calculate degree of agreement using standard inoculums of 10^5 CFUmL^{-1}. The MIC in our case is the lowest concentration of the PS-CaP compound used to restrain the apparent growth of microbes visually after 24 h of incubation at 37°C temperature.

4 RESULTS AND DISCUSSION

The diffusion of electrolytes from a region of higher concentration to a region of lower concentration takes place vigorously when an ionic gradient is maintained between two solutions of varying concentrations of the same electrolyte on either side of the membrane. An electric field is

attained due to the differences in the ionic mobility which are established all throughout the membrane. If the membrane contains large number of negatively charged fixed groups, then the potential gradient will be much larger than the liquid junction potential, which is normally observed when two similar solutions were brought together with or without "uncharged" membrane in between them [21].

The observed values of membrane potentials for the PS-CaP composite were plotted against log $(C_1+C_2)/2$ and are shown in the Fig. 1. It can be seen from the figure that the value of membrane potential observed to be decreased with an increase of electrolyte concentration. This shows that the PS-CaP membrane is negatively charged, i.e. cation selective and its selectivity increases with an increase in dilution due to the structural changes obtained in the electric double layer at the solution-membrane interface [15,17]. In the present case, the observed values of membrane potentials are found to be positive [18] whereas in the case of 3:1 electrolytes, the sign of membrane potential changes from negative to positive [22]. This corresponds to the fact that the membrane is positively charged, i.e. anion selective in the case of 3:1 electrolytes. The change in selectivity character of the membrane is due to the adsorption of multivalent ions leading to a state where net positive charge is left on the membrane surface and thereby making it as anion selective. Therefore, the reversal of surface charge occurs only at 3:1 electrolyte concentration [23].

The generation of a steady electromotive force between two solutions of the same electrolyte differing in their concentration and is separated by a membrane under constant temperature and pressure gradients recognizes the development of some net charge on the membrane. Since, the charge plays a significant role in the two mechanisms like absorption and transportation of simple electrolytes in the model and also in bio-membranes that communicate some considerable electrochemical properties to the membrane, where the most remarkable property is the differences in the permeability of co-ions, counter-ions and neutral molecules. Thus, determining the nature of charges on the membrane is very much important and would be difficult if one proceeds further without any evaluation of thermodynamically effective fixed charge density of the membrane [24].

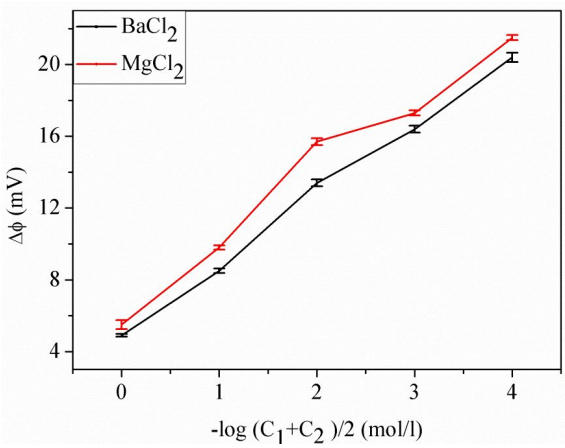

Fig. 1. Plot of total membrane potential (ΔΦ) versus –log (C1+C2)/2 for the PS-CaP membrane when 2:1 electrolytes were used. Each experiment was repeated three times to ensure accuracy of measurements and the data are shown as mean ±SD's of three individual experiments

Nagasawa et al. [12] stated a theory for membrane potentials which is basically based on the charge concept and can also be used for the evaluation of charge density of the membranes. The Nagasawa theory assumes the characteristics such as: (a) the rate determining factor for the permeation of ions and water is the membrane phase, (b) the electrolyte solutions inside and outside the membrane are in thermodynamic equilibrium on either side of the membrane, and (c) the effect of stagnant layer on the permeation velocities is negligible for a thick membrane.

The total membrane potential (ΔΦ) was considered as the sum of diffusion potential ($\Delta\Phi_d$) generally inside the membrane and the electrostatic potential difference ($\Delta\Phi_e$) between the membrane surfaces and the electrolyte solutions on both sides of the membrane. The diffusion potential was obtained by integrating the basic water flow equation for diffusion while the electrostatic potential was calculated according to the Donnan's theory.

$$\Delta\phi = \Delta\phi_d + \Delta\phi_e \tag{6a}$$

where

$$-\Delta\phi_d = -\int_1^2 \frac{J_0 X}{FC_0(C_- + X)U + C_- V}dx + \frac{RT}{F}\int_1^2 \frac{(C_- + X)U}{(C_- + X)U + C_- V}d\ln a_+ - \frac{RT}{F}\int_1^2 \frac{C_- V}{(C_- + X)U + C_- V}d\ln a_- \tag{6b}$$

and

$$-\Delta\phi_e = -\frac{RT}{F}\ln\left(\frac{a_{1+}a_{2+}}{a_1 a_2}\right) \quad (6c)$$

where a_1 and a_2 are the activities of the electrolytes on two sides of the membrane, the + refers to the phenomena occurring in the membrane phase, and J_0 resembles the flow of electrolyte in the absence of electric field; other symbols have their usual significance as stated normally. By integrating eq. (6) using the limit of high electrolyte concentrations through the membrane, the following equation (7) for the membrane potential is obtained:

$$-\Delta\phi = \frac{RT}{F}\left(\frac{X}{2}\right)\left(\frac{\gamma-1}{\gamma}\right)\frac{1}{C_2} + \frac{RT}{F}\left(\frac{U-V}{U+V}\right)\left(\frac{1-XJ_0/RTC_0(U-V)K}{1-XJ_0/2RTC_0VK}\right)\times\ln\gamma + \frac{RT}{2F}\left(\frac{X}{UV}\right)\left(\frac{J_0}{RTC_0K}\right)^2 \left(\frac{1-XJ_0(U+V)/4RTC_0UVK}{1-XJ_0/2RTC_0VK}\right)^2\times[(\gamma-1)C_2]^{-1} \quad (7)$$

At the limit of high electrolyte concentration where the effect of flow of water is negligible, i.e. generally in the absence of an externally applied electric field or pressure gradient, the expression for membrane potential can be written as:

$$-\Delta\phi = \frac{RT}{F}\left(\frac{\gamma-1}{\gamma}\right)\left(\frac{X}{2}\right)\left(\frac{1}{C_2}\right) \quad (8)$$

where γ is the solution-concentration ratio (C_2/C_1) fixed at 10, R is the gas constant, T is the absolute temperature, F is the Faraday constant and X is the charge density on the membrane. Eq. (8) predicts a linear relationship between $\Delta\Phi$ and $(1/C_2)$ and the straight plots shown in Fig. 2 are certainly valid for eq. (8). The values of X derived from the slopes of the linear plots are listed in Table 1. It is quite significant to note that when the charged material is in association with electrolyte solutions, counter ions Cl^- has the opposite charge to that of the material which will obviously generate high concentration within the material as compared to the solution. Whereas as co-ion Ba^+ and Mg^+ will possess the charge same as that of material and it shows less concentration within the material. The fixed charged concentration in the material is basically because of calcium which continuously keeps in touch with hydrated counter ion leading to the formation of ion-pairs on loosing the large amount of water content and on the other hand it repel the co-ions due to the charge that is similar to that of fixed charged group. For maintaining the electrochemical equilibrium between the material and electrolyte solution, the electrical potential difference is initiated of the concentrated charged ion [18]. From the table, it can be observed that that the charge densities for 2:1 electrolytic solutions were found to decrease in the order of $BaCl_2 > MgCl_2$ and that too, the charge densities by the theory was found to be of the same magnitude. It is therefore depicted that the recently developed theoretical equations for the PS-CaP membrane potential are quite similar and so their utility for the evaluation of charge densities of membranes is justified in a very co-ordinated manner at least for the systems under investigation.

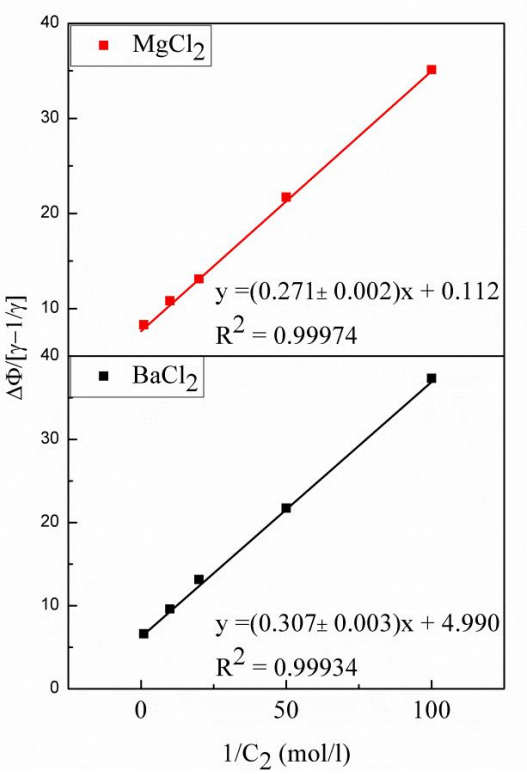

Fig. 2. Plots of $\Delta\phi/[\gamma - 1/\gamma]$ *versus* $1/C_2$ for the PS-CaP membrane using 2:1 electrolytes

Table 1. Charge density derived for the PS-CaP membrane by employing Nagasawa theory

Electrolyte	Nagasawa
	X (eq/l)
$BaCl_2$	0.3077 ± 0.00396
$MgCl_2$	0.2717 ± 0.00221

The dielectric loss tangent is the measurement of irreversibly dissipated energy under the influence of applied electric field and basically consists of the contributions from ionic transport and

relaxation of dipole by the molecular motion. The dielectric loss tangent can be calculated by using the formula given below [25]:

$$\tan\theta = \frac{\varepsilon'}{\varepsilon''} \tag{9}$$

$$\tan\delta = \frac{1}{\tan\theta} = \frac{\varepsilon''}{\varepsilon''} \tag{10}$$

where $\tan\delta$ is the dielectric loss tangent which is proportional to the 'loss' of energy from the applied field into the sample where the energy is dissipated into heat and therefore denoted as dielectric loss. δ is the phase angle between the electric field and the polarization of the dielectric. ε' is the real part of dielectric constant and ε'' is the imaginary part of dielectric constant.

The AC conductivity of the samples can be determined by using the following eq. (11) [26]:

$$\sigma_{ac} = \varepsilon'\varepsilon_0\omega\tan\delta \tag{11}$$

where ω is the angular frequency, ε_0 is the permittivity of the free space.

The real part and imaginary part of impedance were calculated by using the following two formulas:

$$Z' = Z\cos\theta \tag{12}$$

$$Z'' = Z\sin\theta \tag{13}$$

Fig. 3 shows the complex impedance plot of the PS-CaP sample experimented at room temperature. The angular frequency ω increases in an anticlockwise manner on the Z' axis. In general, the grains are effective in the high frequency region, while the grain boundaries are effective in the low frequency region. Thus, the appearance of circular arc in the high frequency region can be due to the contribution from the grain, and the arc in the low frequency region corresponds to the contribution from the grain boundary [27]. It is quite evidential from the plot itself that the Fig. 3 shows single circular arc behaviour, suggesting the predominant nature of grain boundary resistance over the grain resistances in the experimented PS-CaP composite at room temperature.

Fig. 4 shows the variation in dielectric loss factor with frequency for the PS-CaP composite at room temperature. It can be observed from the figure that as the frequency increases, the value of tan δ decreases for the PS-CaP sample. This may be due to the space charge polarization and is considered to be caused by the domain wall resonance. The losses are found to be low since the domain wall motion is inhibited and the magnetization is forced to change the rotation, at higher frequency [28].

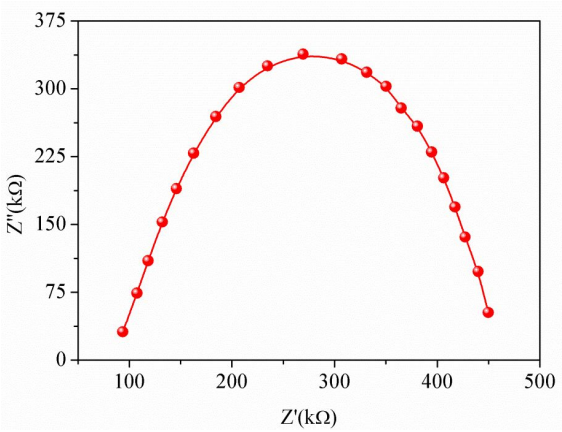

Fig. 3. Cole-Cole plot for the PS-CaP membrane at 298 K temperature

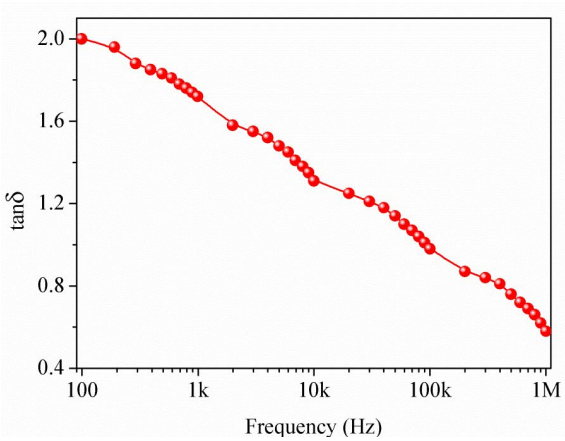

Fig. 4. Plot of $\tan\delta$ *versus* frequency (Hz) for the PS-CaP composite at 298 K temperature

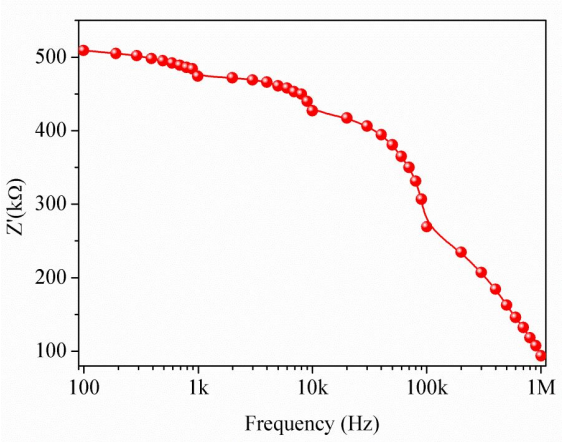

Fig. 5. Plot of Z' *versus* frequency (Hz) for the PS-CaP membrane at 298K temperature

Fig. 5 shows the variation of the real part of impedance (Z') with frequency (Hz) for the PS-CaP membrane. It can be seen clearly from the pattern of the figure that Z' decreases with an increase of frequency for the characterized PS-CaP

sample. For the sample, Z' shows higher values at lower frequencies and decreases simultaneously with increase of frequency, finally attaining a constant value at higher frequency part. This decrease in the real part of impedance for the PS-CaP composite with frequency rise have aroused due to an increase in AC conductivity with respect to the increased frequency [29]. This also indicates that the resistive grain boundaries became conductive because of its intense rise in frequency and finally resembles that the grain boundaries don't even relax at very high frequencies [30].

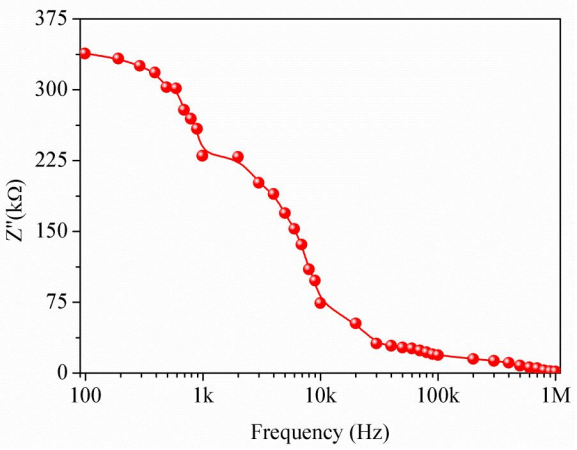

Fig. 6. Plot of Z'' *versus* frequency (Hz) for the PS-CaP composite at 298K temperature.

Similarly, the deviation of imaginary part of impedance (Z'') with frequency (Hz) is shown in Fig. 6, which indicates the same behaviour as similar to Z' in Fig. 5. For the composite, the imaginary part of impedance also found to be decreased with an increase in frequency due to the AC conductivity [31]. From the above evidence it is clear that the PS-CaP material's behaviour is semiconductor in nature.

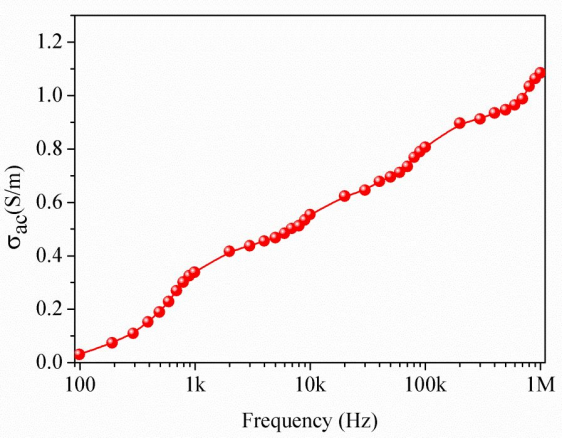

Fig. 7. Plot of σ_{ac} *versus* frequency (Hz) for the PS-CaP composite at 298 K temperature

Fig. 7 shows the variation in AC conductivity with frequency for the PS-CaP composite at room temperature. From the figure, the AC conductivity of the composite found to be increased gradually with an increase of applied field frequency and this is due to the fact that the increased frequency enhances the migration of electrons within the composite [32].

Similarly, the plot of dielectric dispersion (ε'') of the PS-CaP composite as against the applied field frequency (Hz) is shown in Fig. 8. From the figure, the value of ε'' for the PS-CaP composite observed to be decreased with an increase of frequency. At the lower frequencies, the decrease in dielectric constant is rapid and becomes very slow at higher frequencies, which finally approached to a state of frequency independent behaviour [33]. This behaviour of frequency is attributed to the dipole relaxation phenomena. The phenomenon reflects about the delay time of the dipoles subjected to an electric field in response to the frequency. This delay time of dipoles in general occurs due to the inability of dipoles that are responsible for polarization to follow the oscillations of electric field at particular frequencies [34].

Table 2. The PS-CaP composite induced zone of inhibition against (mm) gram positive and gram negative bacterial strain

Compound	Corresponding effect on microorganism (mm)					
	Gram-positive bacteria		Gram-negative bacteria			
	S. mutans	*S. Pyogenes*	MRSA*	*P. aeruginosa*	*S. typhimurium*	*E. coli*
PS-CaP	10.3 ± 0.3	12.8 ± 0.5	15.5 ± 0.4	11.4 ± 0.2	25.3 ± 0.2	15 ± 0.2
Chloramphenicol	25.3 ± 0.4	21.2 ± 0.5	20.5 ± 0.4	15.4 ± 0.2	23.3 ± 0.4	18 ± 0.2
DMSO	-	-	-	-	-	-

*Methicillin resistant *Staphylococcus aureus*
Positive control (chloramphenicol of 30 µg), and negative control (DMSO) measured by the Halo Zone Test (unit, mm).

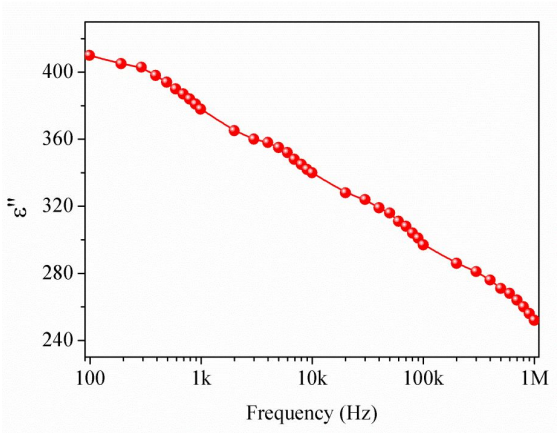

Fig. 8. Plot of dielectric dispersion (ε″) *versus* frequency (Hz) for the PS-CaP membrane at 298K temperature

This is clear from the explanation about the nature of material which shows that the real and the imaginary parts of the dielectric constant of PS-CaP membrane are highly dependent on the frequency behaviour. It also indicates that the dielectric constant decreases with an increase of frequency, i.e. initially decreases randomly and later becoming constant. The dielectric loss of energy also takes place in response to the applied frequency and it also decreases with the increment of frequency. So, it is evidentially clear that if the loss of energy with frequency is less, then it tends to show that the material is very effectual for the experimentation.

From the *in vitro* studies of the PS-CaP composite, the results indicate that the compound to be more active as antimicrobial agent. The PS-CaP treated zone of inhibition were visualized after 24 h of incubation at 37°C against the gram-positive bacteria (*S. mutants, P. aeruginosa*, and MRSA +ve), gram-nevative bacteria (*S. pyogenes, S. typhimurium,* and *E. coli*) and fungi of (*Candida albicans*, *Candida krusei*, *Candida parapsilosis*, and *Cryptococcus neoformans*). The PS-CaP composite induced zones of inhibition (in mm) against the gram-positive and gram-negative bacterial strains are shown in Table-2 and for the fungal strains in Table 4. Similarly, the MIC of the PS-CaP composite for the bacterial and fungal strains are shown in Table.3 and Table 5 respectively. It can be clearly observed from the results that the PS-CaP composite exhibited antibacterial and antifungal activity against all the cultures. For the convenience, we are presenting only two images of antibacterial effect for the proposed zone of inhibition on treatment of the PS-CaP composite. The first image is the antibacterial effect observed with *S. mutants* and the second image is the antifungal effect (*Candida parapsilosis*) observed on treatment of the composite which is shown in the figure 9 (a) and (b).

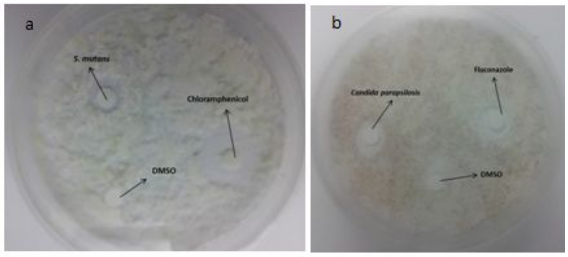

Fig. 9. Antibacterial (a) and antifungal (b) effect observed on *S. mutants* and *Candida parapsilosis* respectively

The higher antimicrobial activity of the PS-CaP compound observed from the results can be easily explained in terms of chelation that makes the metal or polymer complexes to act as more potent and powerful antimicrobial agent, thereby inhibiting the growth of microorganisms [35-36]. It has also been stated that the co-ordination reduces the polarity of polymer ion complexes due to the partial sharing of positive charge with the donor groups within the chelating ring system. This process, in general increases the lipophilic nature of the complex, which favours for the permeability through the lipid bilayer of the microorganism in a more efficient way, thereby destruction of the microorganism in a more aggressive way. Also in our recent report, the cationic charge available on PS in PS-Ti-As caused for a significant decrease in the viability of cardiac cells due to the generation of free radical species and associated intracellular reactions [37]. Similarly, in this case also, the appearance of antibacterial and antifungal activity for the PS-CaP treated composite can be attributed to the cationic effects exhibited by the same PS polymer against the cultures. The interaction of positive charge on PS of the PS-CaP complex with that of the lipid bilayer of microorganism or protein components can mediate many intracellular reactions which are involved in the damage of bacteria and fungi. Therefore, the importance of this work lies in the possibility or the chances that the introduction of new compounds with novel elemental composition might affect the immune responses developed by the generalised bacteria against the traditionally available antimicrobial and antifungal agents. For that, a thorough investigation regarding the structure-activity relationship, toxicity and other biological effects would be beneficial in designing or formulating more potent antimicrobial agents for therapeutic purposes.

5 CONCLUSION

In conclusion, we report the electrochemical, dielectric behaviour and antimicrobial effects of the PS-CaP composite. The composite with good

polymer interaction was prepared by sol-gel process which is an easily adaptive method for membrane synthesis. The experimental results have been well agreed and fulfilled by the Nagasawa approach. By making use of this, we proved that it can be possible to measure the membrane potential, charge density and their quantitative evaluation. The charge density is the central parameter that governs the transport phenomena in membrane phase and it highly depends on the type of electrolytic solution. From the results, the potentials and charge densities for the PS-CaP membrane follows the sequencing order of $BaCl_2$ < $MgCl_2$ and $BaCl_2$ > $MgCl_2$ respectively. The dielectric constant of material shows a frequency dependent variation i.e. the dielectric constant decreased with an increase of applied frequency. Also, the real part of impedance shows a frequency dependent behaviour at very low frequency and it increased rapidly. The comparative *in vitro* antimicrobial studies suggested that the PS-CaP material exhibited significant antibacterial and antifungal activity. For upcoming experimentation, this material model can be enhanced widely to be acceptable and withstand in a range of commercial membranes currently available in the market.

Table 3. Comparison of the MIC of the PS-CaP composite treated bacteria with that of positive control chloramphenicol

Compound	MIC (μg mL^{-1}) Strains					
	Gram-positive bacteria			Gram-negative bacteria		
	S. mutans	*S. Pyogenes*	MRSA*	*P. aeruginosa*	*S. typhimurium*	*E. coli*
PS-CaP	100	100	50	50	50	100
Positive control	16	16	16	16	16	16

*Methicillin resistant *Staphylococcus aureus* (MRSA +ve);

Table 4. Comparison of the zone of inhibition of the PS-CaP composite treated fungi with that of positive and negative controls

Compound	Corresponding effect on microorganism			
	CA	CK	CP	CN
PS-CaP	14.5± 0.4	11.5± 0.2	10.5± 0.7	8.9 ± 0.5
Fluconazole	19.3± 0.5	15.5± 0.4	12.5± 0.5	10.5± 0.4
DMSO	-	-	-	-

CA, *Candida albicans*; CK, *Candida krusei*; CP, *Candida parapsilosis*, CN, *Cryptococcus neoformans.*
Positive control (fluconazole of 30 μ g), and negative control (DMSO) measured by the Halo Zone Test (unit, mm).

Table 5. Comparison of the MIC of the PS-CaP composite treated fungi with that of positive control of fluconazole

Compound	MIC (μg mL^{-1}) strains			
	CA	CK	CP	CN
PS-CaP	100	100	100	100
Positive Control	1	32	4	4

Acknowledgements

The authors would like to thank the respective departments and universities for the financial support in order to complete this project.

Reference

[1] W. den Hollander, P. Patka, C.P. Klein and G.A. Heidendal, 1991. Macroporous calcium phosphate ceramics for bone substitution:a tracer study on biodegradation with 45Ca tracer, Biomaterials, vol. 12, pp. 569 – 73. DOI: 10.1016/0142-9612(91)90053-D

[2] (a)T. Arfin and Rafiuddin, 2012. Metal ion transport through a polystyrene-based cobalt arsenate membrane: application of irreversible thermodynamics and theory of absolute reaction rates, Desalination, vol. 284, pp. 100-105. DOI: 10.1016/j.desal.2011.08.042

(b) T. Arfin and Rafiuddin, 2010. Thermodynamics of ion conductivity of alkali halides across a polystyrene-based titanium arsenate membrane, Electrochim. Acta, vol. 55, pp. 8628-8631. DOI: 10.1016/j.electacta.2010.07.091

[3] (a) G.S. Gohil, R.K. Nagarale, V.V. Binsu and V.K. Shahi, 2006. Preparation and characterization of monovalent cation selective sulfonated poly (ether ether ketone) and poly (ether sulfone) composite membranes, J. Colloid Interface Sci. vol. 298, pp. 845-853. DOI: 10.1016/j.jcis.2005.12.069

(b) T. Arfin and N. Yadav, 2013. Impedance characteristics and electrical double-layer capacitance of composite polystyrene-cobalt-arsenate membrane, J. Ind. Eng. Chem., vol. 19, pp. 256-262. DOI: 10.1016/j.jiec.2012.08.009

[4] (a) T.J. Chou and A. Tanioka, 1998. Ionic behaviour across charged membranes in methanol water solutions. I: Membrane potential, J. Membr. Sci., vol. 144, pp. 275-284. DOI: 10.1016/S0376-7388(98)00069-6

(b) T. Arfin and F. Mohammad, 2013. DC electrical conductivity of nano-composite polystyrene-titanium-arsenate membrane,

J. Ind. Eng. Chem., vol. 19, pp. 2046-2051. DOI: 10.1016/j.jiec.2013.03.019

[5] M.N. Beg, F.A. Siddiqi, A. Husain and B. Islam, 1979. Preparation of cupric palmitate membrane, its characterization and evaluation of thermodynamically effective fixed charge density, Lipids, vol. 14, pp. 682-686. DOI:10.1007/BF02533455

[6] Z.D. Deng and K.A. Mauritz, 1992. Dielectric relaxation studies of acid-conducting short side-chain perfluorosulfonate ionomer membranes, Macromolecules, vol. 25, pp. 2369-2380. DOI: 10.1021/ma00086a016

[7] P.C. Appelbaum and P.A. Hunter, 2000. The fluoroquinolone antibacterials: past, present and future perspectives, Int. J. Antimicrob. Ag., vol. 16, pp. 5-15. DOI: 10.1016/S0924-8579(00)00192-8

[8] (a) S.J. Brickner, D.K. Hutchinson, M.R. Barbachyn, P.R. Manninem, D.A. Ulanowicz, S.A. Garmon, K.C. Grega, S.K. Hendges, D.S. Toops, C.W. Ford and G.E. Zurenko, 1996. Synthesis and antibacterial activity of U-100592 and U-100766, two oxazolidinone antibacterial agents for the potential treatment of multidrug-resistant gran-positive bacterial infections, J. Med. Chem., vol. 39, pp. 673-679. DOI: 10.1021/jm9509556
(b) V.T. Andriole, J. Remington, M. Swartz, M.A. Malden, Current Clinical Topics in Infectious Diseases, Blackwell Sciences, 1998, pp. 18-19. ISBN 0-6320-4402-0

[9] (a) V. Snaz-Nebot, I. Valls, D. Barbero and J. Barbosa, 1997. Acid-base behaviour of quinolones in aqueous acetonitrile mixtures, Acta Chem. Scand., vol. 28, pp. 896-903. DOI:10.1002/chin.199751161
(b) J.A. Vazquez, V. Sanchez, C. Dmuchowski, L.M. Dembry, J.D. Sobel and M.J. Zervos, 1998. Nosocomial acquisition of candida albicans: an epidemiologic study, J. Infect. Dis., vol. 168, pp. 195-201. DOI: 10.1093/infdis/168.1.195

[10] M.A. Pfaller and D.J. Diekema, 2007. Epidemiology of invasive candidiasis: a persistent public health problem, Clin. Microbiol. Rev., vol. 20, pp.133-163. DOI: 10.1128/CMR.00029-06

[11] A.N. Sudjana, C.F. Carson, K.C. Carson, T.V. Riley and K.A. Hammer, 2012. Candida albicans adhesion to human epithelial cells and polystyrene and formation of biofilm is reduced by sub-inhibitory melaleuca alternifolia (tea tree) essential oil, Med. Mycol., vol. 50, pp. 863-870. DOI: 10.3109/13693786.2012.683540

[12] M. Tasaka, N. Aoki, Y. Konda and M. Nagasawa, 1975. Membrane potentials and electrolyte permeation velocities in charged membranes, J. Phys. Chem., vol. 79, pp. 1307-1314. DOI: 10.1021/j100580a017

[13] F.A. Siddiqi, M.N. Beg and P. Prakash, 1979. Studies with model membranes. XXII. Evaluation of thermodynamic parameters and testing of theories of membrane and bi-ionic potential based on nonequilibrium thermodynamics, J. Polym. Sci., vol. 17, pp. 539-550. DOI: 10.1002/pol.1979.170170223

[14] T. Arfin and S. Fatima, 2013. Conductometric studies with polystyrene calcium phosphate membrane, Asian J. Adv. Basic Sci., vol. 2, pp.1-14.

[15] T. Arfin, F. Jabeen and R.J. Kriek, 2011. An electrochemical and theoretical comparison of ionic transport through a polystyrene based titanium-vanadium (1:2) phosphate membrane, Desalination, vol. 274, pp. 206-211. DOI: 10.1016/j.desal.2011.02.014

[16] T. Arfin and Rafiuddin, 2009. Electrochemical properties of titanium arsenate membrane, Electrochim. Acta, vol. 54, pp. 6928-6934. DOI: 10.1016/j.electacta.2009.06.074

[17] (a) T. Arfin and N. Yadav, 2012. Impedance characteristics and electrical double layer capacitance of polystyrene based nickel arsenate membrane, Anal. Bioanal. Electrochem., vol. 4, pp. 135-152.
(b) T. Arfin, R. Bushra and R.J. Kriek, 2013. Ionic conductivity of alkali halides across a polyaniline-zirconium(IV)-arsenate membrane, Anal. Bioanal. Electrochem., vol. 5, pp. 206-221.

[18] (a) T. Arfin and Rafiuddin, 2011. An electrochemical and theoretical comparison of ionic transport through a polystyrene-based cobalt arsenate membrane, Electrochim. Acta, vol. 56, pp. 7476-7483. DOI: 10.1016/j.electacta.2011.06.109
(b) T. Arfin and Rafiuddin, 2009. Transport studies of nickel arsenate membrane, J. Electroanaly. Chem., vol. 636, pp.113-122. DOI: 10.1016/j.jelechem.2009.09.019

[19] T. Arfin, A. Falch and R.J. Kriek, 2012. Evaluation of charge density and the theory for calculating membrane potential for a nano-composite nylon-6,6 nickel

phosphate membrane, Phys. Chem. Chem. Phys., vol. 14, pp.16760-16769. DOI: 10.1039/C2CP42683H

[20] (a) R. Cruickshank, J.P. Duguid, B.P. Marmion and R.H.A. Awain, 1995. Medicinal Microbiology, 12th ed., vol.11, Churchill Livingstone, London, pp. 196. (b) T.J. Mackie, Mackie and McCartney, 1989. Practical Medical Microbiology, 13th ed., Churchill Livingstone, Edinburgh, pp. 696.

[21] S.A. Khan, K. Saleem, and Z. Khan, 2007. Synthesis, characterization and in vitro antibacterial activity of new steroidal thiazolo quinoxalines, Eur. J. Med. Chem., vol. 42, pp.103-108. DOI: 10.1016/j.ejmech.2006.07.006

[22] G.S. Gohil, V.K. Shahi and R. Rangarajan, 2004. Comparative studies on electrochemical characterization of homogeneous and heterogeneous type of ion-exchange membrane, J. Membr. Sci., vol. 240, pp. 211-219. DOI: 10.1016/j.memsci.2004.04.022

[23] K. Singh and A.K. Tiwari, 2004. Studies on electrochemical characterization of membranes, Proc. Ind. Natl. Sci. Acad., vol. 70, pp.477-482.

[24] K. Singh, A.K. Tiwari and J.P. Rai, Alumina membrane supported on a polyvinylidene fluoride matrix, Ind. J. Chem., vol. 24, pp.825-827

[25] M.N. Beg and M.A. Matin, 2005. Studies with nickel phosphate membranes: evaluation of charge density and test of recently developed theory of membrane potential, J. Membr. Sci., vol. 196, pp. 201-209. DOI: 10.1016/S0376-7388(01)00582-8

[26] M. Thambidurai, N. Muthukumarasamy, D. Velauthapillai, S. Agilan and R. Balasundaraprabhu, 2012. Impedance spectroscopy and dielectric properties of cobalt doped CdS nanoparticles, Powder Technol., vol.217, pp. 1-6. DOI: 10.1016/j.powtec.2011.09.038

[27] A.M.M. Farea, S. Kumar, K.M. Batoo, A. Yousef, C.G. Lee and Alimuddin, 2008. Structure and electrical properties of $Co_{0.5}Cd_xFe_{2.5-x}O_4$ ferrites, J. Alloy Compd., vol. 464, pp.361-369. DOI: 10.1016/j.jallcom.2007.09.126

[28] (a) D.C. Onwudiwe, T. Arfin, C.A. Strydom and R.J. Kriek, 2013. A study of the thermal and AC impedance properties of N-phenyldithiocarbamate complexes of Zn (II), Electrochim. Acta, vol. 109, pp. 809-817. DOI: 10.1016/j.electacta.2013.07.176 (b) D.C. Onwudiwe, T. Arfin, C.A. Strydom and R.J. Kriek, 2013. Synthesis, spectroscopic characterization and behaviour of AC impedance spectroscopy of Cd (II) bis (N-para-methylphenyl dithiocarbamate), Electrochim. Acta, vol. 104, pp. 19-25. DOI: 10.1016/j.electacta.2013.04.081

[29] T. Kar and R.N.P. Choudhary, 1997. Structural dielectric and electrical properties of LiNbMoO6 ceramics, Mater. Lett., vol. 32, pp.109-113. DOI: 10.1016/S0167-577X (97)00014-1

[30] M.E. Orazem and B. Tribollet, 2008. An integrated approach to electrochemical impedance spectroscopy, Electrochim. Acta, vol. 53, pp.7360-7366. DOI: 10.1016/j.electacta.2007.10.075

[31] N.K. Singh, P. Kumar and R. Rai, 2011. Comparative study of structure, dielectric and electrical behaviour of Ba(Fe0.5Nb0.5)O3 ceramics and their solid solutions with BaTiO3, Adv. Mater. Lett., vol. 2, pp. 200-205. DOI: 10.5185/amlett.2010.11178

[32] A.N. Jansen, P.T. Wojcik, P. Agarwal and M.E. Orazem, 1996. Thermally-stimulated deep-level impedance spectroscopy: application to an n-GaAs Schottky diode, J. Electrochem. Soc., vol. 143, pp. 4066-4074. DOI: 10.1149/1.1837337

[33] T. Šalkus, V. Galeckas, J.C. Badot, I.I. Makauz, I.P. Studenyak, A. Selskis, A. Kežionis and J. Banys, Impedance spectroscopy study of Cu6PS5I-As2S3 nanocomposites, Ionics, vol. 19, pp.1387-1391. DOI: 10.1007/s11581-013-0875-4

[34] J.F. Jurado, J.A. Trujillo, B.-E. Mellander and R.A. Vaegas, 2003. Effect of AgBr on the electrical conductivity of (-AgI, Solid State Ionics, vol. 156, pp.103-112. DOI: 10.1016/S0167-2738(02)00614-8

[35] A. Chamola, H. Singh and U.C. Naithani, Study of Pb(Zr0.65Ti0.35)O3(PZT(65/35) doing on structural, dielectric and conductivity properties of BaTiO3(BT) ceramics, Adv. Mater. Lett., vol. 2, pp. 148-152. DOI: 10.5185/amlett.2010.11183

[36] E. Berejo, R. Carballo, A. Castiñeiras, R. Dominguez, C. Maiche-Mössmer, J. Strähle and D.X. Best, 1999. Synthesis, characterization and antifungal activity of group 12 metal complexes of 2-acetylpyridine-4N-ethylthiosemicarbazone (H4EL) and 2-acetylpyridine-N-oxide-4N-ethylthiosemicarbazone (H4ELO) Polyhedron, vol. 18, pp. 3695-3702. DOI: 10.1016/S0277-5387(99)00309-5

[37] Z.H. Chohan, A. Scozzafava and C.T. Supuran, 2003. Zinc complexes of benzothiazole-derived Schiff bases with antibacterial activity, J. Enzyme Inhib. Med. Chem., vol. 18, pp. 259-263.
DOI: 10.1080/1475636031000071817

[38] F. Mohammad andT. Arfin, 2013. Cytotoxic effects of polystyrene-titanium-arsenate composite in cultured H9c2 cardiomyoblasts, Bull. Environ. Contam. Tox., vol. 91, pp. 689-696.
DOI:10.1007/s00128-013-1131-3